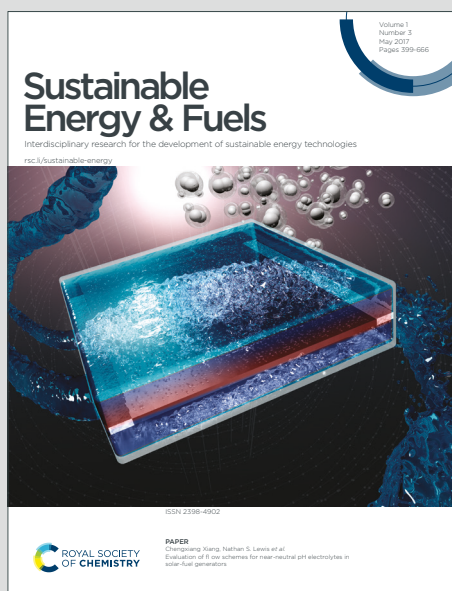


# Sustainable Energy & Fuels

Interdisciplinary research for the development of sustainable energy technologies

Accepted Manuscript

This article can be cited before page numbers have been issued, to do this please use: D. Zakgeym, J. Hofmann, L. Maurer, F. Auer, K. Müller, M. Wolf and P. Wasserscheid, *Sustainable Energy Fuels*, 2023, DOI: 10.1039/D2SE01750D.



This is an Accepted Manuscript, which has been through the Royal Society of Chemistry peer review process and has been accepted for publication.

Accepted Manuscripts are published online shortly after acceptance, before technical editing, formatting and proof reading. Using this free service, authors can make their results available to the community, in citable form, before we publish the edited article. We will replace this Accepted Manuscript with the edited and formatted Advance Article as soon as it is available.

You can find more information about Accepted Manuscripts in the [Information for Authors](#).

Please note that technical editing may introduce minor changes to the text and/or graphics, which may alter content. The journal's standard [Terms & Conditions](#) and the [Ethical guidelines](#) still apply. In no event shall the Royal Society of Chemistry be held responsible for any errors or omissions in this Accepted Manuscript or any consequences arising from the use of any information it contains.

# Better Through Oxygen Functionality?

## The Benzophenone/Dicyclohexylmethanol LOHC-System

View Article Online  
DOI: 10.1039/D2SE01750D

Dina Zakgeym,<sup>a,b</sup> Jonas David Hofmann,<sup>a</sup> Lukas Maurer,<sup>a</sup> Franziska Auer,<sup>a</sup> Karsten Müller,<sup>c</sup>  
Moritz Wolf,<sup>d</sup> Peter Wasserscheid<sup>a,b,\*</sup>

<sup>a</sup> Helmholtz-Institut Erlangen-Nürnberg für Erneuerbare Energien (IEK 11),  
Forschungszentrum Jülich GmbH, Erlangen, Germany

<sup>b</sup> Friedrich-Alexander-Universität Erlangen-Nürnberg (FAU), Lehrstuhl für Chemische  
Reaktionstechnik, Erlangen, Germany

<sup>c</sup> University of Rostock, Institute of Technical Thermodynamics, Rostock, Germany

<sup>d</sup> Karlsruhe Institute of Technology (KIT), Engler-Bunte-Institute & Institute of Catalysis  
Research and Technology, Karlsruhe, Germany

\*Corresponding author. Address: Cauerstr. 1, 91058 Erlangen, Germany. E-Mail-address:  
[p.wasserscheid@fz-juelich.de](mailto:p.wasserscheid@fz-juelich.de)

**Abstract**View Article Online  
DOI: 10.1039/D2SE01750D

Storage in liquid organic hydrogen carriers (LOHCs) constitutes a safe and infrastructure-compatible way to transport and handle hydrogen. To date, widely studied LOHC-systems are often differentiated into nitrogen-containing systems, such as N-ethylcarbazole (H0-NEC)/perhydro-N-ethylcarbazole (H12-NEC), or heteroatom-free LOHC systems, such as toluene/methylcyclohexane, benzyltoluene (H0-BT)/perhydro-benzyltoluene (H12-BT) and dibenzyltoluene (H0-DBT)/perhydro-dibenzyltoluene (H18-DBT). In this contribution we introduce the oxygen-containing LOHC system benzophenone/dicyclohexylmethanol, a system that is characterized by an excellent hydrogen storage capacity of 7.19 mass% or 2252 Wh/L. We herein demonstrate that benzophenone (H0-BP) can be selectively and completely hydrogenated to dicyclohexylmethanol (H14-BP, perhydro-benzophenone) over Ru/Al<sub>2</sub>O<sub>3</sub> catalysts at 50 bar hydrogen pressure and temperatures in the range of 90 to 180 °C. Hydrogen can be released from H14-BP using Pt-based catalysts to form H0-BP at temperatures of 250 °C. Depending on the catalyst support, undesired dehydration to diphenylmethane may become relevant with acidic supports favoring dehydrative water removal from the molecule. Most remarkably, Cu-based catalysts, such as the well-known commercial methanol synthesis catalyst, show excellent activity in the selective transformation of H14-BP to dicyclohexylketone (H12-BP) at surprisingly mild conditions. This enables hydrogen release of 1/7 of the stored hydrogen at temperatures as low as 170 °C.

**Keywords:**

LOHC systems, hydrogen storage, benzophenone, dicyclohexylmethanol, dehydration, copper-zinc

## 1. Introduction

A future sustainable and fully defossilized energy system can only be achieved if renewable sources, such as solar, wind and hydropower, are coupled with large-scale and long-term energy storage technologies. These can compensate for fluctuations in energy availability, which are typically associated with renewable sources, and facilitate transport from locations with high energy harvesting potential to locations with high energy demand. One concept for energy storage is the utilization of surplus energy for water electrolysis, yielding oxygen and green hydrogen.<sup>[1]</sup> At suitable times and locations, the stored energy can be released, e.g. in a fuel cell, where the stored hydrogen and oxygen from air react back to water in a cold combustion process to produce electrical power. However, the storage and transport of molecular hydrogen is not a trivial task, as the established physical storage technologies, such as high pressure or liquefaction, require new and costly logistics infrastructure.<sup>[2–4]</sup>

These challenges may be addressed by methods of chemical hydrogen storage. Among those, liquid organic hydrogen carriers (LOHCs) are characterized by the fact that a fuel-like organic molecule is charged with hydrogen in an exothermal catalytic hydrogenation reaction. After storage and transport of the hydrogenation product, hydrogen can be released on demand.<sup>[2,4,5]</sup> The resulting LOHC-systems thus consist of a pair of organic molecules, the hydrogen-lean form of the system and the hydrogen-rich form of the system. For systems with more than one aromatic group in their hydrogen-lean LOHC compound, also partially hydrogenated molecules form part of the respective LOHC system and these intermediates are in many systems important for melting point depression. It is an important aspect of all LOHC technologies that existing infrastructure from traditional fossil fuel-based energy distribution technologies may be reused, at least to some part, to reduce infrastructure cost for establishing a future green hydrogen economy.<sup>[1,3,4]</sup>

Table 1 compares well-studied LOHC pairs by giving important physico-chemical characteristics of the hydrogen-lean compound. Besides the hydrocarbon systems based on toluene, benzyltoluene (H0-BT) and dibenzyltoluene (H0-DBT), the nitrogen-containing LOHC system based on N-ethylcarbazole (H0-NEC) has been investigated in detail.<sup>[5]</sup>

**Table 1:** Melting point  $T_m$ , boiling point  $T_b$ , hydrogen capacity, liquid density  $\rho$  and enthalpy of hydrogenation at 25 °C of four well-studied, hydrogen-lean LOHC compounds: toluene, benzyltoluene (H0-BT), dibenzyltoluene (H0-DBT), N-ethylcarbazole (H0-NEC) and benzophenone (H0-BP).

LOHC	$T_m$ [°C]	$T_b$ [°C]	H <sub>2</sub> capacity [mass%]	$\rho$ [g cm <sup>-3</sup> ]	$\Delta_r H_m$ [kJ mol(H <sub>2</sub> ) <sup>-1</sup> ]
Toluene	- 95 <sup>[6]</sup>	111 <sup>[6]</sup>	6.16	0.87 <sup>a</sup> [6]	- 68 <sup>[5]</sup>
H0-BT	- 30 <sup>[7]</sup>	280 <sup>[7]</sup>	6.22	1.00 <sup>a</sup> [8]	- 63 <sup>[8]</sup>
H0-DBT	- 39 to - 34 <sup>[7]</sup>	390 <sup>[7]</sup>	6.24	1.04 <sup>a</sup> [8]	- 65 <sup>[8]</sup>
H0-NEC	68 <sup>[7]</sup>	270 <sup>[7]</sup>	5.83	1.06 <sup>b</sup> [9]	- 50 <sup>[5]</sup>

<sup>a</sup> at 20 °C      <sup>b</sup> at 75 °C

The given properties should be shortly discussed with regard to their relevance for a real-life high performance hydrogen storage technology: i) A low melting point enables operation of the LOHC storage system at cold temperatures without storage tank heating; ii) high boiling temperatures of the hydrogen-lean LOHC compounds make purification of the released hydrogen by simple condensation of the LOHC vapor much easier; iii) high hydrogen capacity allows to ship a given mass of hydrogen in a smaller mass of LOHC; iv) high LOHC density enables higher volumetric storage density at the same mass-based hydrogen capacity; v) low enthalpy of hydrogenation enables dehydrogenation at lower temperatures which is a very relevant point as the endothermal hydrogen release requires heat input and lower dehydrogenation temperatures facilitate heat integration and reduce heat losses.

Compared to its pure hydrocarbon counterparts, the nitrogen-containing LOHC system based on H0-NEC bears the advantage of a significantly lower heat of dehydrogenation (Table 1).<sup>[5,10]</sup> The system has, however, the disadvantage of lower compatibility with the fuel infrastructure (N-containing fuels are hardly used today), higher toxicity,<sup>[11]</sup> and lower thermal stability.<sup>[5,10]</sup>

In contrast, the handling of oxygen-containing organic compounds in the fuel infrastructure is well known. Examples include the biofuel components ethanol, fatty acid esters (biodiesel) and methyl-tert-butylether that is used as anti-knock agent. It is, therefore, somewhat surprising that oxygen-containing LOHC systems have not been investigated so far. Among the few exceptions are theoretical studies in the academic and patent literature.<sup>[12,13]</sup> Moreover, the LOHC system

acetone/isopropanol has been recently described for direct electrochemical hydrogen utilization using direct organic fuel cells.<sup>[14–17]</sup>

Herein, we show that oxygen-containing LOHC systems offer indeed exceptionally high hydrogen storage capacities, very attractive low-temperature hydrogen release performance and very attractive features for potential technical applications if oxygen-functionalities and cycloalkyl/aromatic moieties are combined in their molecular structure. We exemplify this structural concept for the LOHC system benzophenone (H0-BP)/dicyclohexylmethanol (H14-BP) as shown in Figure 1.

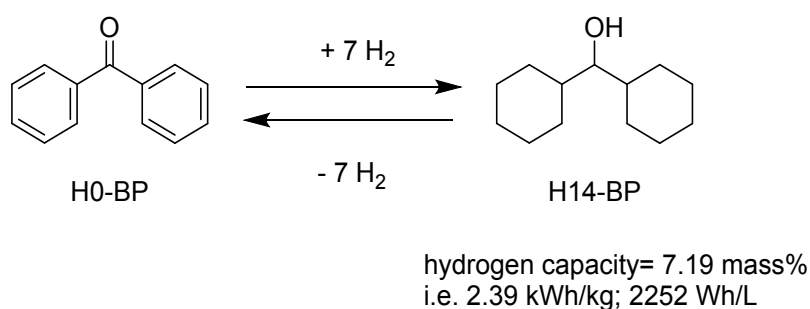


**Figure 1:** Hydrogen storage in the LOHC system benzophenone/dicyclohexylmethanol.

The storage cycle involves 7 hydrogen molecules of which one is provided by the dehydrogenation of the secondary alcohol function and six are provided by the dehydrogenation of the two cyclohexyl rings. In total, a hydrogen storage capacity of 7.19 mass% is realized which is 17% higher than that of methylcyclohexane, H12-BT and H18-DBT, and even 23 % higher than that of H12-NEC. Looking at the volumetric storage density, the high liquid density of H14-BP (density at 60 °C is 0.94 g/mL)<sup>[18]</sup> increases this capacity advantage even further. Liquid H14-BP carries 2252 Wh/L compared to 1507 Wh/L for methylcyclohexane, 1760 Wh/L for H12-BT, 1848 Wh/L for H18-BT and 1774 Wh/L for H12-NEC (all data compared at 60 °C).

Note that the melting points of both benzophenone and dicyclohexylmethanol are 48 and 58 °C, respectively. Thus, handling these LOHC compounds in pure form requires some heating of the tank system. Alternatively, these LOHC compounds may be handled at lower temperatures as liquids in form of eutectic mixtures, e.g. with other LOHC compounds. This concept of melting point suppression has been in the past very successfully applied for H0-NEC (a compound melting equally at 58 °C). Here it has been found that mixtures with other N-alkylcarbazoles provide melting points below room temperature. Similar concepts may be applicable for the here described H0-BP/H14-BP LOHC system.

Prior to such technical fine tuning, it is important, however, to show first that the H0-BP/H14-BP LOHC system can indeed serve as reversible hydrogen storage system. For this purpose, hydrogenation and dehydrogenation kinetics studies and stability investigations are required. These investigations are reported in this contribution. Most remarkably, we found that 1/7 of the hydrogen stored in H14-BP is very easily released at very mild conditions with the help of a technical Cu-based catalyst. This finding enables interesting start-up options for providing hydrogen from the described LOHC system in more flexible manner.

## 2. Experimental

### 2.1. Materials

Benzophenone (H0-BP, 99%, Sigma Aldrich, B9300) was used as received. Cyclohexane (>99.8%, 1.00667.1000, Merck) and acetone (>99.8%, 34850, Sigma Aldrich) were used as solvents for the LOHC compounds and reaction mixtures to avoid solidification after cooling to room temperature. All catalysts applied in this work were purchased from commercial sources: Ru/Al<sub>2</sub>O<sub>3</sub> (5 mass%) from Sigma Aldrich (LOT: 439916), Pt/C (5 mass%) from Sigma Aldrich (LOT: 205931), Pt/Al<sub>2</sub>O<sub>3</sub> (0.3 mass%, EleMax D101) from Clariant, and CuO/ZnO/Al<sub>2</sub>O<sub>3</sub> (50.9 mass% Cu) from Alfa Aesar (LOT: I06Z036).

### 2.2. Hydrogenation

The hydrogenation of H0-BP was carried out in a 300 mL alloy C-276 autoclave (Parr Instrument). The autoclave was equipped with a gas entrainment impeller, thermocouple, argon line, internal cooling coil, rupture disk and a liquid phase sampling line with a filter. A perfluoroelastomer (FFKM) sealing ring was used due to its high chemical resistance against (partially) hydrogenated and aromatic benzophenone species (Hx-BP) as well as (partially) hydrogenated and aromatic diphenylmethane (Hx-DPM) species.

In a typical experiment, the autoclave was charged with 164 g H0-BP and 1.82 g Ru/Al<sub>2</sub>O<sub>3</sub>, which corresponds to a LOHC:Ru molar ratio of 1000:1. The reactor was purged three times with argon (3 bar) and then heated up to 90 °C under continuous stirring at 425 rpm. The stirring rate was increased to 1200 rpm after adding hydrogen pressure of 50 bar at the desired hydrogenation temperature to ensure contact between catalyst, reactant and the gas phase. The reaction was carried out in semi-batch mode under constant pressure. Liquid samples were acquired via the sampling line every 30, 60 or 120 min depending on the reaction time. Approximately 0.2 mL of the effluent liquid from the sampling line were discarded to avoid

contamination with the previous sample. Afterwards, approximately 0.05 mL were collected for the off-line GC analysis.

View Article Online  
DOI: 10.1039/D2SE01750D

After full hydrogenation was reached as confirmed by GC analysis, the H14-BP was dissolved in cyclohexane, filtered to remove the catalyst from the solution and transferred into a flask. The cyclohexane was removed in a rotary evaporator at 60 °C and a pressure of 80 mbar yielding H14-BP with a purity of approximately 98% according to GC analysis (1.7 mass% of H12-DPM being the major impurity).

### 2.3. Dehydrogenation

H14-BP was dehydrogenated in a stirred 100 mL semi-batch glass apparatus equipped with a heating mantle. Temperature control was achieved with a type K thermocouple inside the reaction mixture connected to a fitron 4 TP temperature controller (Fiege electronic). A custom-made stainless steel tube connected to the glass flask allowed the addition of pre-filled catalyst at reaction temperature while keeping the apparatus isolated from the ambient environment. The reaction mixture as well as the catalyst in the tube were overflowed by 200 mL min<sup>-1</sup> argon using an EL-FLOW Prestige mass flow controller (MFC; Bronkhorst). A reflux condenser (15 °C) mitigated discharge of volatile organic compounds through the gas phase. Argon flow and temperature were controlled by the Flow View software (Bronkhorst, V1.23) and a custom-built fitron TP software (V1.0.2b), respectively.

In a typical dehydrogenation reaction, 29.75 g H14-BP (purity 98%, corresponding to 0.15 mol) were heated up under argon while stirring at 500 rpm with a magnetic bar. Upon reaching the desired reaction temperature, the catalyst tube was opened to add the pre-weighed catalyst to the reaction mixture. Liquid samples were extracted by a syringe puncturing a septum on the glass apparatus and filtered through a syringe filter with a pore size of 0.20 μm. Samples were taken immediately after the start of the reaction and every 30 or 60 min depending on the reaction time.

### 2.4. Gas chromatography analysis of liquid samples and calculation of liquid-phase molar fractions and product selectivities

All samples taken to monitor the reaction progress in both, hydrogenation and dehydrogenation, were analyzed via GC. For this purpose, the sample was diluted with acetone and analyzed in a Trace 1310 gas chromatograph from Thermo Scientific with a SRxi17Sil column (30 m, inner

diameter 0.25 mm) and detected by means of an FID. For this, 1.0  $\mu\text{L}$  of the sample was injected and evaporated at 250  $^{\circ}\text{C}$ , whereby the split ratio was 1:150. The carrier gas was helium with a flow rate of 1.0  $\text{mL min}^{-1}$ . The optimized temperature program applied to obtain good separation of all products of either hydrogenation of H0-BP or dehydrogenation of H14-BP included heating to 110  $^{\circ}\text{C}$  (holding time: 5 min), followed by heating with 10  $^{\circ}\text{C}/\text{min}$  to 130  $^{\circ}\text{C}$  (holding time: 5 min), followed by heating with 5  $^{\circ}\text{C}/\text{min}$  to 145  $^{\circ}\text{C}$  (holding time: 10 min), followed by heating with 5  $^{\circ}\text{C}/\text{min}$  to 180  $^{\circ}\text{C}$  (holding time: 0 min) and followed by heating with 10  $^{\circ}\text{C}/\text{min}$  to 270  $^{\circ}\text{C}$  (holding time: 5 min).

Before and after each series of measurements, the column was purged by injecting acetone as described above, heating the column from 100 to 300  $^{\circ}\text{C}$  within 2 minutes with a holding time of 5 minutes. All chromatograms were displayed by the Thermo Xcalibur Qual Browser software (version 4.0.27.19). The molar fraction  $n_i/n_{tot}$  of each reactant or product in the liquid phase was calculated from its integral  $A_i$  and its molar mass  $M_i$  using a calibration factor  $f_i$  (Equation (1)). The selectivity towards a product  $i$  was calculated from its molar fraction and the molar fraction of reactant H14-BP in the liquid phase (Equation (2)).

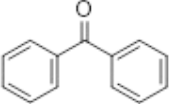
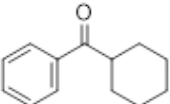
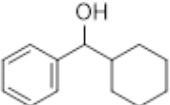
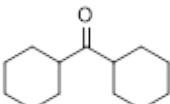
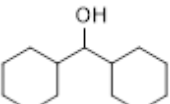
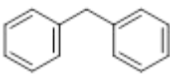
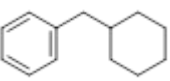
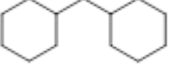
$$\frac{n_i}{n_{tot}} = \frac{\frac{A_i f_i}{M_i}}{\sum_j \frac{A_j f_j}{M_j}} \quad (1)$$

$$S_i = \frac{\frac{n_i}{n_{tot}}}{1 - \frac{n_{H14-BP}}{n_{tot}}} \quad (2)$$

The identity of all compounds detected in the GC was confirmed using mass spectrometry (MS) ensuring inclusion of all relevant isomers. The corresponding MS data can be found in the ESI (Table SI-1). All relevant reaction intermediates and (side) products as well as the used abbreviations are summed up in Table 2.

**Table 2:** Structures and abbreviations for all relevant reaction intermediates and (side) products in the hydrogenation/dehydrogenation of H0-/H14-BP.

View Article Online  
DOI: 10.1039/D2SE01750D

Compound name	Structure	Abbreviation
Benzophenone		H0-BP
Cyclohexylphenylmethanone		H6-BP
Cyclohexylphenylmethanol		H8-BP
Dicyclohexylketone		H12-BP
Dicyclohexylmethanol		H14-BP
Diphenylmethane		H0-DPM
Cyclohexylmethylbenzene		H6-DPM
Dicyclohexylmethane		H12-DPM

### 3. Results and discussion

#### 3.1. Selective hydrogenation of H0-BP

The catalytic hydrogenation of H0-BP proceeds via three different hydrogenation pathways that are displayed in Figure 2. In pathway (1), the keto functionality is first hydrogenated to the secondary alcohol followed by hydrogenation of the two aromatic rings to the final product H14-BP. Alternatively (2), the hydrogenation of the two aromatic rings can proceed first and the ketone hydrogenation as the last step. The third way (3) includes the hydrodeoxygenation (HDO) of H0-BP as first step, which represents a well-known reaction from the literature.<sup>[19]</sup> The so-obtained diphenylmethane (H0-DPM) is then hydrogenated to dicyclohexylmethane

(H12-DPM). Note, that HDO is an unwanted side reaction in the H0-BP/H14-BP storage cycle as the HDO of one H0-BP molecule consumes two mols of hydrogen, one for the water formation and one for the saturation of the carbon structure of the Hx-BP. As indicated in Figure 2 by the dotted lines, HDO can occur from every Hx-BP intermediate as well as from the H14-BP product. This reaction has to be suppressed by the right choice of catalyst and reaction conditions to enable efficient hydrogen storage and release.

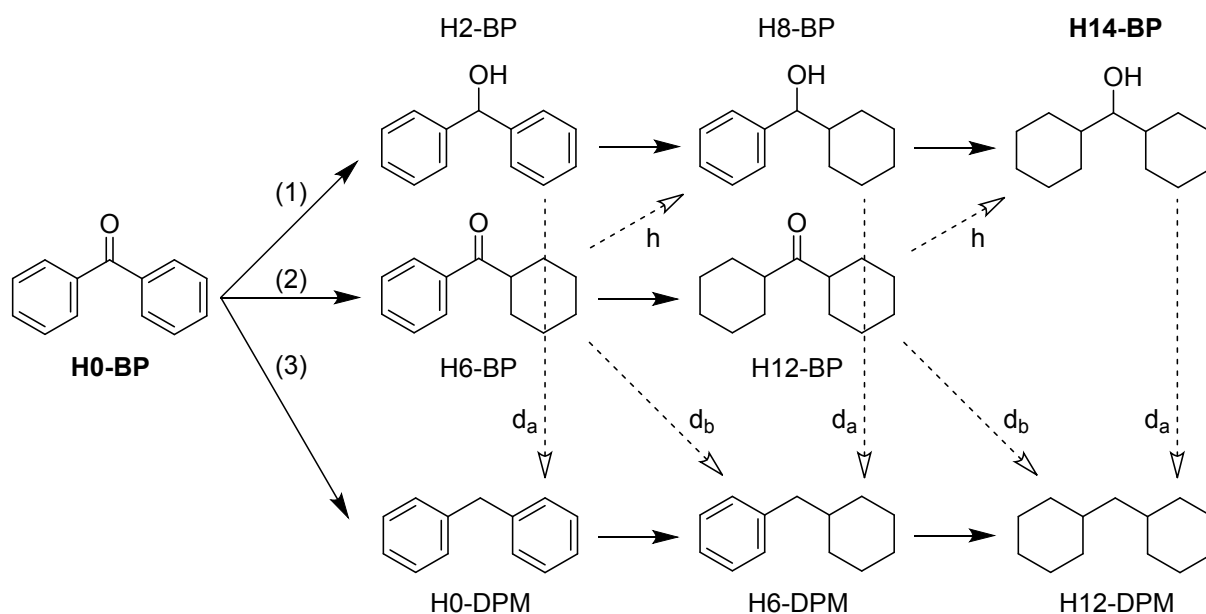


**Figure 2:** Reaction network in the catalytic hydrogenation of H0-BP to the desired product H14-BP; (1) pathway where ketone hydrogenation proceeds first; (2) pathway where aromatic group hydrogenation proceeds first; (3) pathway where the undesired hydrodeoxygenation proceeds first; possible connections between the pathways are indicated by dotted lines. Hydrogen and product water have been omitted for clarity.

For our hydrogenation studies we selected three commercial catalyst materials, namely, Ru/Al<sub>2</sub>O<sub>3</sub>, Pt/C and Pt/Al<sub>2</sub>O<sub>3</sub>. The hydrogenation experiments were initially carried out at 180 °C and a hydrogen pressure of 50 bar in a batch reactor. The detailed product distributions as a function of reaction time can be found in the Electronic Supplementary Information (ESI) for each catalyst under investigation (Figure SI-1 to SI-3). Figure 3 shows the final yields of H12-BP, H14-BP and H12-DPM after the total reaction time of 24 h. It is seen that for all three catalyst systems under investigation, the formation of H12-DPM is significant, for Pt/C the reaction even shows a high selectivity for this undesired pathway. Note, that the sum of yields for H12-BP and H14-BP was >97% only in the case of Ru/Al<sub>2</sub>O<sub>3</sub> and Pt/C. The hydrogenation of H0-BP with Pt/Al<sub>2</sub>O<sub>3</sub> was quite slow, in contrast, with only 60% combined yield of H12-BP and H14-BP after 24 h reaction time.

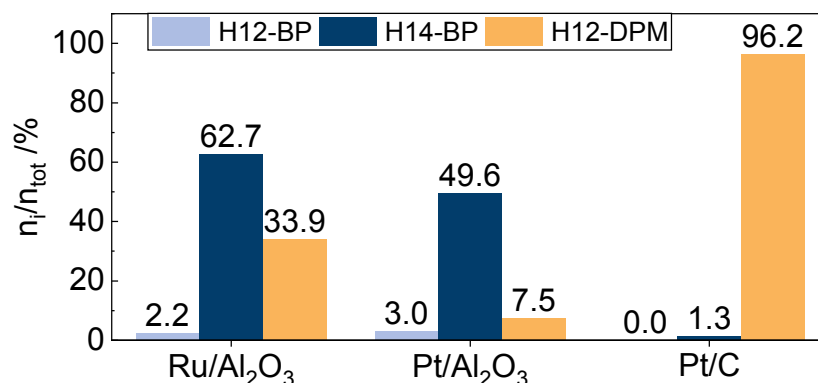


**Figure 3:** Liquid phase molar product fractions of H12-BP, H14-BP and H12-DPM after hydrogenation of H0-BP for 24 h at 180 °C and 50 bar H<sub>2</sub> with different catalysts; further conditions: H0-BP:metal = 1000:1.

As the Ru-based catalyst showed the highest selectivity to the desired hydrogenation product H14-BP, this catalyst was selected for a further optimization of the reaction conditions. Therefore, the reaction temperatures were varied between 90 and 180 °C, while maintaining a constant hydrogen partial pressure of 50 bar. The detailed product distributions as a function of reaction time can again be found in the ESI (Figure SI-4 to SI-6). Figure 4 shows the molar fractions of the main products H14-BP, H12-BP and H12-DPM after 24 h reaction time. Notably, the reaction temperature has a strong effect on the obtained selectivity. While the undesired, deoxygenated compound H12-DPM represents about a third of the product mixture at 180 °C, its molar fraction declines significantly with lower temperatures indicating a higher Arrhenius activation energy of HDO compared to the catalytic hydrogenation reaction. Interestingly, the selectivity for the desired H14-BP reaches 98% at a reaction temperature of 90 °C demonstrating the feasibility of a highly selective H0-BP hydrogenation unleashing the full potential of the high hydrogen storage capacity of >7 mass%.

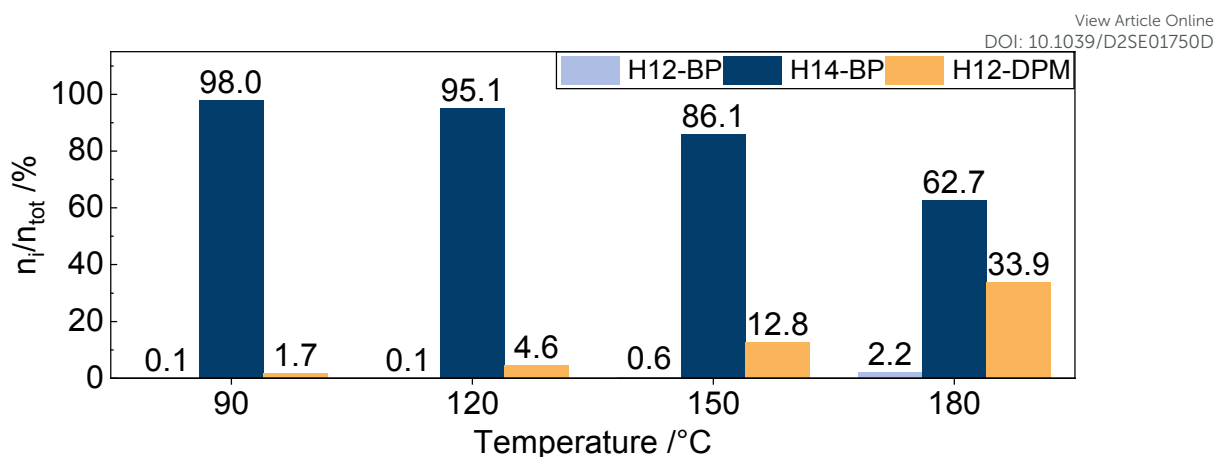


**Figure 4:** Liquid phase molar product fractions of H12-BP, H14-BP and H12-DPM after hydrogenation of H0-BP for 24 h at various reaction temperatures and 50 bar H<sub>2</sub>; further conditions: 5 mass% Ru/Al<sub>2</sub>O<sub>3</sub>, H0-BP:metal = 1000:1.

### 3.2. Dehydrogenation of H14-BP

The catalytic dehydrogenation of H14-BP may also proceed via three routes as shown in Figure 5: A first dehydrogenation pathway (1) involves dehydrogenation of the secondary alcohol function as the first step. Alternatively, the dehydrogenation of the two cyclohexyl rings proceeds first (2). Dehydration to form oxygen-free LOHC species is the first step in the third pathway (3). Again, dehydration is a possible path for each of the formed H<sub>x</sub>-BP species and every mole of H<sub>x</sub>-BP that liberates water reduces the hydrogen yield by two moles of hydrogen. Possible side reactions of the components in the reaction mixture involve formation of aldol condensation products (by addition of H14-BP and H12-BP) and deep dehydrogenation to fluorenol or fluorenone. Aldol condensation, however, is rather unlikely due to the steric shielding of the oxygen-functionalities in H<sub>x</sub>-BP.<sup>[20]</sup>

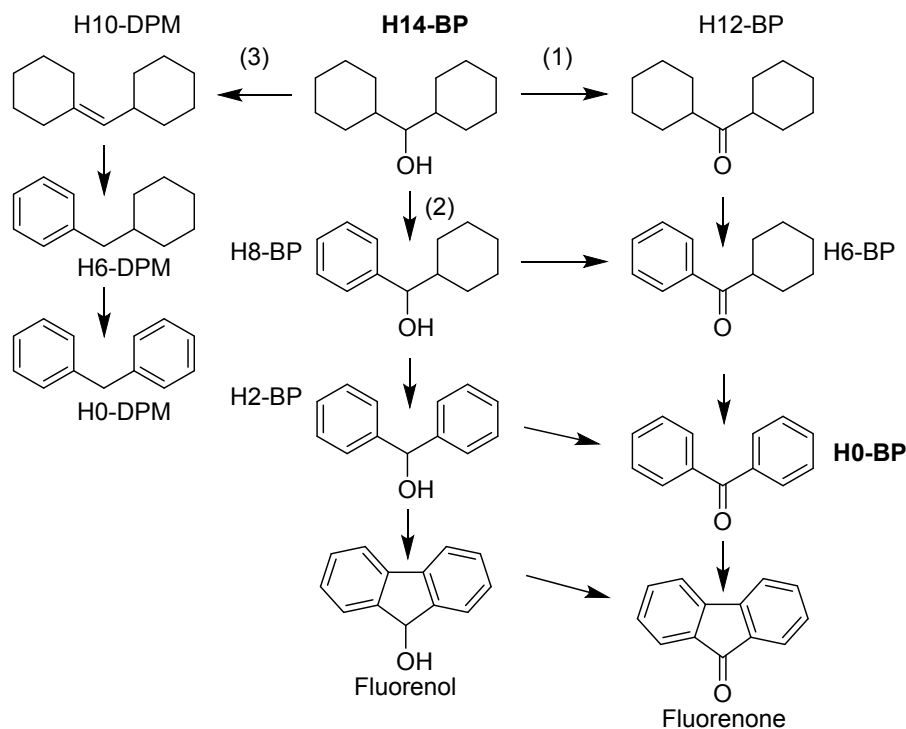


**Figure 5:** Potential reaction sequences in the catalytic dehydrogenation of H14-BP to the desired product H0-BP: (1) pathway where alcohol dehydrogenation proceeds first; (2) pathway where cyclohexyl group dehydrogenation proceeds first; (3) pathway where the undesired dehydration proceeds first; possible further connections between the pathways by dehydration of other Hx-BP species as well as hydrogen and product water have been omitted for clarity.

In our catalytic studies, the dehydrogenation of H14-BP was first tested at 230 °C using Ru/Al<sub>2</sub>O<sub>3</sub> (Figure 6) as its activity for hydrodeoxygenation and dehydration has been found low in the hydrogenation experiments. Interestingly, a selectivity of 96% to H12-BP was achieved. Only traces of H12-DPM and H6-DPM (below 2%) were detectable, but also no formation of any aromatic product was observed. The rate of H12-BP formation was quite high, leading to a molar fraction of 56% after 5 h.

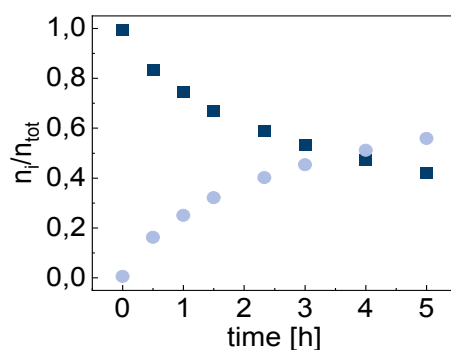


**Figure 6:** Liquid phase molar fractions of reactant and products in the dehydrogenation of H14-BP at 230 °C using 5 mass% Ru/Al<sub>2</sub>O<sub>3</sub>; further conditions: 0.15 mol H14-BP; 200 mL min<sup>-1</sup> argon flow, 0.15 mmol Ru; H14-BP (■) and H12-BP (●).

In the next step, Pt/Al<sub>2</sub>O<sub>3</sub> (Figure 7a), which is the most commonly used catalyst for the dehydrogenation of H18-DBT and H12-BT,<sup>[21–26]</sup> was applied. For comparison, Figure 7b shows the same experiment with a commercial Pt/C catalyst to highlight reactivity differences caused by the nature of the catalyst support material.

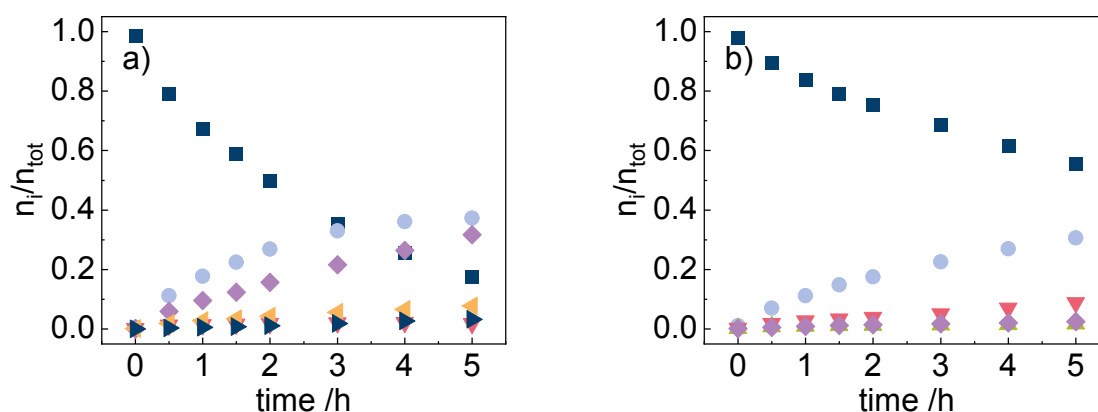


**Figure 7:** Liquid phase molar fractions of reactant and products in the dehydrogenation of H14-BP at 230 °C using a) 0.3 mass% Pt/Al<sub>2</sub>O<sub>3</sub> and b) 5 mass% Pt/C; further conditions: 0.15 mol H14-BP; 200 mL min<sup>-1</sup> argon flow; H14-BP (■), H12-BP (●), H8-BP (▲), H6-BP (▼), H12-DPM (◀), H6-DPM (◆), H0-DPM (▶).

The comparison shows that the main reaction over both catalysts is indeed the dehydrogenation of the hydroxyl group to the corresponding ketone H12-BP. This reaction is responsible for hydrogen release from oxygen functionalized LOHCs under mild conditions and proceeds faster over Pt/Al<sub>2</sub>O<sub>3</sub> than over Pt/C. Regarding further ring dehydrogenation, the formation of H6-BP is observed to some extent with Pt/C, but insignificantly with Pt/Al<sub>2</sub>O<sub>3</sub>. As little to no H8- and H2-BP are observed, reaction pathway (1) (Figure 5) is assumed to be dominant. The undesired dehydration (pathway (3), Figure 5), however, appears primarily with the alumina supported Pt catalyst as indicated by the significant formation of H6-DPM. The splitting off of the oxygen functionality therefore most probably takes place via dehydration followed by rapid hydrogen rearrangement and ring dehydrogenation. This reaction sequence occurs competitively to the desired dehydrogenation. For Pt/Al<sub>2</sub>O<sub>3</sub> also the formation of H12-DPM is observed showing that dehydration followed by hydrogenation is a possible reaction sequence that consumes two moles of the produced hydrogen per mole of H12-DPM formed.

Based on the identified intermediates and products with these two Pt catalysts, the reaction sequence may be simplified (Figure 8) taking into account that ring dehydrogenation prior to ketone formation is irrelevant. All reactions are assumed to be reversible, except for the deoxygenation of H14-BP to H6-DPM.

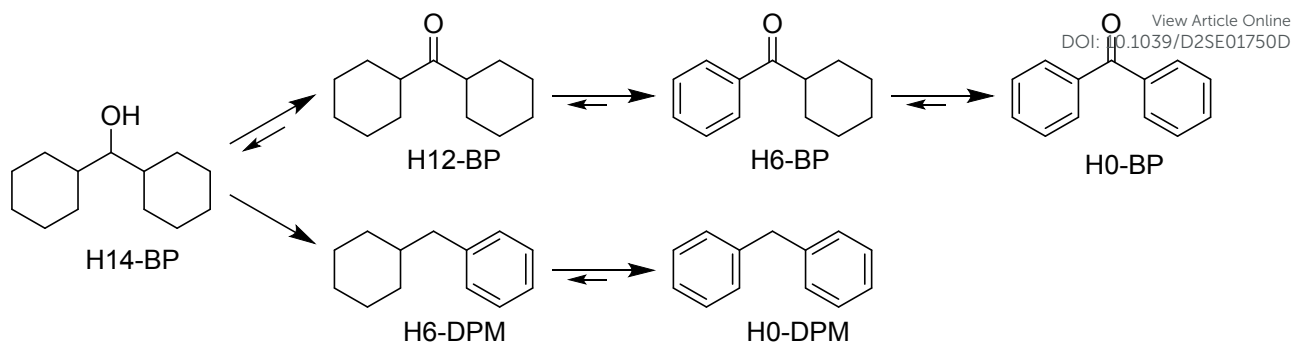


**Figure 8:** Identified main reaction pathways in the catalytic dehydrogenation of H14-BP with Pt/Al<sub>2</sub>O<sub>3</sub> and Pt/C; hydrogen and product water have been omitted for clarity.

Other noble metal catalysts (Pd, Ir, Rh) were tested as well, but only showed minor activity (see ESI Figure SI-7). To our great surprise, we found that the commercial methanol synthesis catalyst, CuO/ZnO/Al<sub>2</sub>O<sub>3</sub>, is an excellent catalyst for the selective dehydrogenation of H14-BP to H12-BP. The catalyst outperforms by far all applied precious metal systems, although the Cu to LOHC molar ratio was higher (1:60) than in the case of Pt or Ru (1:1000) reflecting the much lower price of Cu vs. the applied precious metals. Already after 30 min reaction time, the remaining molar ratio of H14-BP was below 5% with almost 100% selectivity to H12-BP formation (Figure 9).

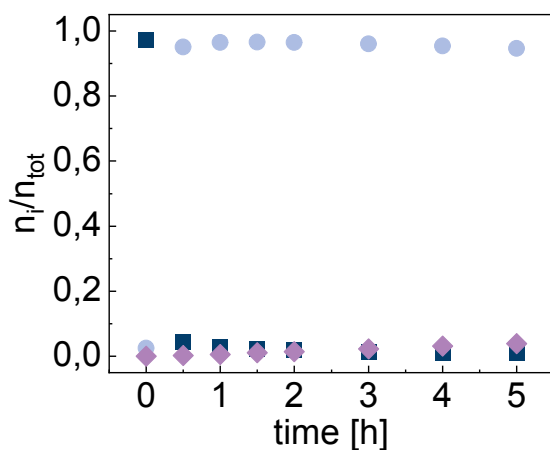


**Figure 9:** Liquid phase molar fractions of reactant and products in the dehydrogenation of H14-BP at 230 °C using CuO/ZnO/Al<sub>2</sub>O<sub>3</sub>; further conditions: 0.15 mol H14-BP; 200 mL min<sup>-1</sup> argon flow, 2.5 mmol Cu; H14-BP (■) and H12-BP (●), H6-DPM (◆).

### 3.3. Temperature influence on dehydrogenation of H14-BP over CuO/ZnO/Al<sub>2</sub>O<sub>3</sub>

View Article Online

DOI: 10.1039/D2SE01750D

In order to study the highly interesting catalytic activity of CuO/ZnO/Al<sub>2</sub>O<sub>3</sub> in H14-BP dehydrogenation in more detail, we performed a temperature variation study with this catalyst in the range between 150 and 210 °C and more frequent sampling.

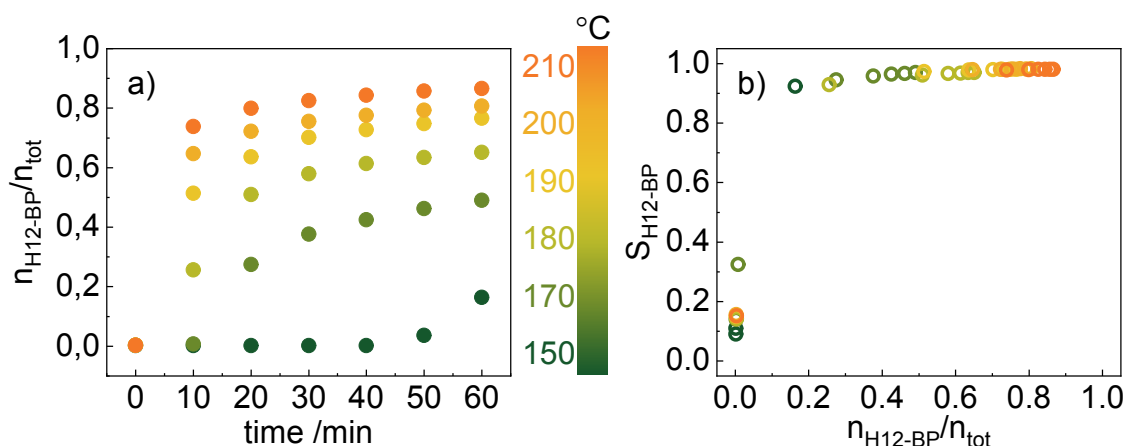


**Figure 10:** a) Liquid phase molar fractions of H12-BP over reaction time and b) selectivity towards H12-BP as a function of H12-BP concentration in the dehydrogenation of H14-BP using CuO/ZnO/Al<sub>2</sub>O<sub>3</sub> at various temperatures: 0.15 mol H14-BP; 200 mL min<sup>-1</sup> argon flow, 2.5 mmol Cu.

Remarkably, significant dehydrogenation activity is obtained even at a temperature as low as 150 °C. At only 170 °C, full dehydrogenation to H12-BP is found after a reaction time of 24 h (see ESI Figure SI-8). However, at these low temperatures a preforming effect of the catalyst could be observed. At 170 °C the reaction started only 10 min after catalyst addition, while at 150 °C no reaction progress was observed until 40 min after the start of the experiment. This hints toward a self-activation of the catalyst at the reaction start. The catalytic dehydrogenation of H14-BP exhibited excellent selectivities in the investigated temperature range (Figure 10b). Only at very small H12-BP concentrations (i.e. low reaction progress), the selectivity determination was influenced by impurities in the reactant H14-BP (especially H12-DPM). However, at higher H12-BP yields the selectivity exceeded 95%. No other products than H12-BP and Hx-DPM (less than 1 % of all products) were found in the product mixture.

### 3.4. Temperature influence on dehydrogenation of H14-BP over Pt/C

Because no sign of the desired formation of H6-BP and H0-BP was found using the CuO/ZnO/Al<sub>2</sub>O<sub>3</sub> catalyst, we continued our experimental studies by a variation of reaction temperature with the Pt/C catalyst, the catalyst system with the most promising selectivity in

the dehydrogenation reaction of H14-BP. The temperature variation was carried out in the range from 220 to 250 °C (Figure 11).

View Article Online  
DOI: 10.1039/C2SE01750D

Detailed plots of all reaction products over time are shown in the ESI (Figure SI-9). Here we focus on a comparison of the two main reaction pathways shown in Figure 8, dehydrogenation to Hx-BP compounds and dehydrogenation combined with hydrodeoxygenation leading to Hx-DPM compounds. It is noteworthy, that the evolution of the dehydrogenation products follows the expected temperature dependent first-order type kinetics while the evolution of the deoxygenated products increases in an almost linear manner at all investigated temperatures. Therefore, it is possible to identify reaction times where a high degree of dehydrogenation still goes hand-in-hand with moderate hydrodeoxygenation. For the case of the experiment at 250 °C this  $t_{opt}$  is 1 h and the optimum ration of products<sub>dehydr.</sub> / products<sub>dehydr+hydrodeoxy.</sub> was found to be 6.99.

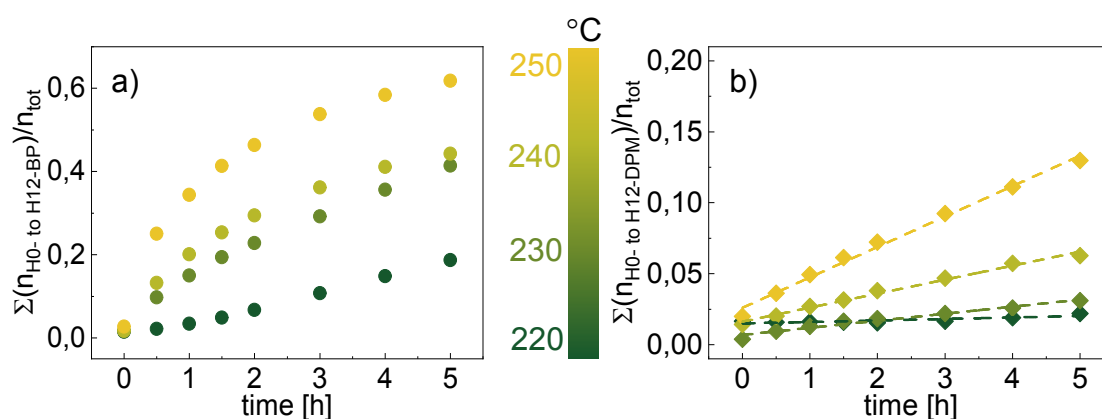


**Figure 11:** Temperature variation in the H14-BP dehydrogenation with Pt/C (5 mass%): a) combined liquid phase molar fractions of the dehydrogenation products H0-BP, H2-BP, H6-BP, H8-BP, H12-BP; b) combined liquid phase molar fractions of the dehydrogenation + hydrodeoxygenation products H0-DPM, H6-DPM, H12-DPM; conditions: 0.15 mol H14-BP, 200 mL min<sup>-1</sup> argon. Dashed lines represent a linear fit to guide the eye.

### 3.5. Thermodynamics considerations for the dehydrogenation of H14-BP

Dehydrogenation of H14-BP comprises two types of hydrogen release reactions: the dehydrogenation of a secondary alcohol forming a ketone and the dehydrogenation of alicyclic rings forming aromatic rings. While thermodynamics of the latter step are similar to the dehydrogenation of conventional LOHCs, such as methylcyclohexane or perhydro-benzyltoluene, dehydrogenation of the secondary alcohol function is characterized by somewhat different thermochemical parameters. Enthalpy of reaction for liquid phase reaction

is basically the same, within the margin of uncertainty, for both reaction types (+68.1 kJ mol<sup>-1</sup>(H<sub>2</sub>) for H14-BP → H12-BP compared to +67.6 kJ mol<sup>-1</sup>(H<sub>2</sub>) for H12-BP → H0-BP; data estimated using the method by Domalski and Hearing<sup>[33]</sup>). View Article Online  
DOI: 10.1039/D2SE01750D

The experimental observation that H12-BP is preferably formed in the reaction, while reaction products with dehydrogenated rings are far less prominent in the reaction mixture, is consistent with the thermochemical properties of the respective reactions. Dehydrogenation of the secondary alcohol is thermodynamically more favorable in the open, two-phase system of the experiments described above. However, the fact that dehydrogenation of rings is primarily observed for molecules with a carbonyl group rather than with a hydroxyl group should not be attributed to thermodynamics, but rather to a kinetic effect in the catalytic reaction. The reaction system has not reached equilibrium and a certain share of those molecules that undergo dehydrogenation of the alcohol can directly undergo ring dehydrogenation, while being adsorbed onto the catalyst surface.

#### 4. Conclusion

The potential of H0-BP/H14-BP as novel LOHC system has been investigated. We demonstrated that the full hydrogen storage capacity of 7.19 mass% can be realized by hydrogenation of benzophenone at 90 °C and 50 bar of hydrogen using Ru/Al<sub>2</sub>O<sub>3</sub> as catalyst. While the hydrogenation reaction with Ru/Al<sub>2</sub>O<sub>3</sub> yielded H14-BP with a selectivity exceeding 98%, the same reaction with Pt/C and Pt/Al<sub>2</sub>O<sub>3</sub> showed undesired hydrodeoxygenation to a significant extent.

The hydrogen release reaction from H14-BP includes the thermodynamically favored formation of the H12-BP ketone with release of one mole of hydrogen per mol of H14-BP. This reaction can proceed in a highly selective manner with Ru/Al<sub>2</sub>O<sub>3</sub> and CuO/ZnO/Al<sub>2</sub>O<sub>3</sub>. The alcohol dehydrogenation was found to be very fast with CuO/ZnO/Al<sub>2</sub>O<sub>3</sub> showing significant activity down to 150 °C and complete conversion and full yield of H12-BP within less than 30 min. This very active reaction may open pathways for low temperature partial dehydrogenation of H14-BP or two-step dehydrogenation sequences. Only the use of Pt catalysts, however, showed significant dehydrogenation of the alicyclic rings of H14-BP enabling full release of the stored hydrogen. Also during dehydrogenation, the loss of the oxygen-containing group by hydrodeoxygenation is the main undesired side reaction as two moles of hydrogen are consumed during the formation of one mole of water from any of the H<sub>x</sub>-BP species in the reaction system. Further catalyst development is necessary to mitigate deoxygenation especially

during dehydrogenation to make full use of the outstanding hydrogen storage capacity of the H0-BP/H14-BP LOHC system.

View Article Online  
DOI: 10.1039/D2SE01750D

### **Conflicts of interest**

Peter Wasserscheid is founder and minority shareholder of the company Hydrogenious LOHC technologies ([www.hydrogenious.net](http://www.hydrogenious.net)) that offers commercially hydrogen storage systems based on the LOHC technology.

There is no conflict of interest to declare with regard to the specific scientific results reported in this paper.

### **Acknowledgements**

This work was funded by the Bavarian Ministry of Economic Affairs, Regional Development and Energy through the project “Emissionsfreier und stark emissionsreduzierter Bahnverkehr auf nicht-elektrifizierten Strecken”.

## References

View Article Online  
DOI: 10.1039/D2SE01750D

- [1] P. Preuster, A. Alekseev, P. Wasserscheid, *Annu. Rev. Chem. Biomol. Eng.* **2017**, *8*, 445–471.
- [2] M. Niermann, S. Drünert, M. Kaltschmitt, K. Bonhoff, *Energy Environ. Sci.* **2019**, *12*, 290–307.
- [3] K. Müller, *ChemBioEng Rev.* **2019**, *6*, 72–80.
- [4] M. Jang, Y. S. Jo, W. J. Lee, B. S. Shin, H. Sohn, H. Jeong, S. C. Jang, S. K. Kwak, J. W. Kang, C. W. Yoon, *ACS Sustain. Chem. Eng.* **2019**, *7*, 1185–1194.
- [5] P. Preuster, C. Papp, P. Wasserscheid, *Acc. Chem. Res.* **2017**, *50*, 74–85.
- [6] Institut für Arbeitsschutz der Deutschen Gesetzlichen Unfallversicherung, “GESTIS-Stoffdatenbank,” can be found under <https://gestis.dguv.de/search>, **2021**.
- [7] N. Brückner, K. Obesser, A. Bösmann, D. Teichmann, W. Arlt, J. Dungs, P. Wasserscheid, *ChemSusChem* **2014**, *7*, 229–235.
- [8] K. Müller, K. Stark, V. N. Emel’yanenko, M. A. Varfolomeev, D. H. Zaitsau, E. Shoifet, C. Schick, S. P. Verevkin, W. Arlt, *Ind. Eng. Chem. Res.* **2015**, *54*, 7967–7976.
- [9] K. Stark, V. N. Emel’yanenko, A. A. Zhabina, M. A. Varfolomeev, S. P. Verevkin, K. Müller, W. Arlt, *Ind. Eng. Chem. Res.* **2015**, *54*, 7953–7966.
- [10] K. Müller, *CBEN* **2019**, cben.201900009.
- [11] M. Markiewicz, Y. Q. Zhang, A. Bösmann, N. Brückner, J. Thöming, P. Wasserscheid, S. Stolte, *Energy Environ. Sci.* **2015**, *8*, 1035–1045.
- [12] K. Paragian, B. Li, M. Massino, S. Rangarajan, *Mol. Syst. Des. Eng.* **2020**, *5*, 1658–1670.
- [13] G. P. Pez, A. R. Scott, A. C. Cooper, H. Cheng, F. C. Wilhelm, A. H. Abdourazak, *Hydrogen Storage by Reversible Hydrogenation of Pi-Conjugated Substrates*, **2008**, US7351395.
- [14] G. Sievi, D. Geburtig, T. Skeledzic, A. Bösmann, P. Preuster, O. Brummel, F. Waidhas, M. A. Montero, P. Khanipour, I. Katsounaros, J. Libuda, K. J. J. Mayrhofer, P. Wasserscheid, *Energy Environ. Sci.* **2019**, *12*, 2305–2314.
- [15] P. Hauenstein, D. Seeberger, P. Wasserscheid, S. Thiele, *Electrochem. Commun.* **2020**, *118*, 106786.
- [16] S. Auffarth, W. Dafinger, J. Mehler, V. Ardizzon, P. Preuster, P. Wasserscheid, S. Thiele, J. Kerres, *J. Mater. Chem. A* **2022**, *10*, 17208–17216.
- [17] P. Hauenstein, I. Mangoufis-Giasin, D. Seeberger, P. Wasserscheid, K. J. J. Mayrhofer, I. Katsounaros, S. Thiele, *Journal of Power Sources Advances* **2021**, *10*, 100064.
- [18] D. Zakgeym, Katalysator- Und Prozessentwicklung Für Sauerstoffhaltige Flüssige Organische Wasserstoffträger-Systeme, PhD Thesis, Friedrich-Alexander-Universität Erlangen-Nürnberg (FAU), **2022**.
- [19] M. Bejblová, P. Zámotný, L. Červený, J. Čejka, *Applied Catalysis A: General* **2005**, *296*, 169–175.
- [20] K. P. C. Vollhardt, N. E. Schore, H. Butenschön, B. Elvers, *Organische Chemie*, Wiley-VCH, Weinheim, **2009**.
- [21] F. Auer, A. Hupfer, A. Bösmann, N. Szesni, P. Wasserscheid, *Catal. Sci. Technol.* **2020**, *10*, 6669–6678.
- [22] S. Dürr, S. Zilm, M. Geißelbrecht, K. Müller, P. Preuster, A. Bösmann, P. Wasserscheid, *Int. J. Hydrog. Energy* **2021**, DOI 10.1016/j.ijhydene.2021.07.119.
- [23] S. Mrusek, P. Preuster, K. Müller, A. Bösmann, P. Wasserscheid, *Int. J. Hydrog. Energy* **2021**, *46*, 15624–15634.

- [24] A. Bulgarin, H. Jorschick, P. Preuster, A. Bösmann, P. Wasserscheid, *Int. J. Hydrog. Energy* **2020**, *45*, 712–720. View Article Online  
DOI: 10.1039/D2SE01750D
- [25] F. Auer, D. Blaumeiser, T. Bauer, A. Bösmann, N. Szesni, J. Libuda, P. Wasserscheid, *Catal. Sci. Technol.* **2019**, *9*, 3537–3547.
- [26] T. Rüde, S. Dürr, P. Preuster, M. Wolf, P. Wasserscheid, *Sustainable Energy Fuels* **2022**, *6*, 1541–1553.
- [27] G. A. M. Hussein, N. Sheppard, M. I. Zaki, R. B. Fahim, *J. Chem. Soc., Faraday Trans. 1* **1989**, *85*, 1723–1741.
- [28] A. Gervasini, A. Auroux, *J. Catal.* **1991**, *131*, 190–198.
- [29] E. Jasińska, B. Krzyżyńska, M. Kozłowski, *Catal. Lett.* **2008**, *125*, 145–153.
- [30] S. S. M. Konda, S. Caratzoulas, D. G. Vlachos, *ACS Catal.* **2016**, *6*, 123–133.
- [31] K. Larmier, C. Chizallet, S. Maury, N. Cadran, J. Abboud, A.-F. Lamic-Humblot, E. Marceau, H. Lauron-Pernot, *Angew. Chem. Int. Ed.* **2017**, *56*, 230–234.
- [32] K. Larmier, C. Chizallet, N. Cadran, S. Maury, J. Abboud, A.-F. Lamic-Humblot, E. Marceau, H. Lauron-Pernot, *ACS Catal.* **2015**, *5*, 4423–4437.
- [33] E. S. Domalski, E. D. Hearing, *J. Phys. Chem. Ref. Data* **1993**, *22*, 805–1159.